

Effect of oxygen content on the transport properties and magnetoresistance in $[\text{Ca}_2\text{CoO}_{3-\delta}]_{0.62}[\text{CoO}_2]$ single crystals

X. G. Luo, X. H. Chen*, G. Y. Wang, C. H. Wang, Y. M. Xiong, H. B. Song, H. Li and X. X. Lu
*Hefei National Laboratory for Physical Science at Microscale and Department of Physics,
University of Science and Technology of China, Hefei, Anhui 230026, People's Republic of China*
(Dated: November 20, 2018)

Transport property is investigated in $[\text{Ca}_2\text{CoO}_{3-\delta}]_{0.62}[\text{CoO}_2]$ single crystals obtained by varying annealing conditions. The $\rho_{ab}(T)$ exhibits a resistivity minimum, and the temperature corresponding to this minimum increases with the loss of oxygen content, indicative of the enhancement of spin density wave (SDW). Large negative magnetoresistance (MR) was observed in all single crystals $[\text{Ca}_2\text{CoO}_{3-\delta}]_{0.62}[\text{CoO}_2]$, while a magnetic-field-driven insulator-to-metal (IM) transition in oxygen annealed samples. These results suggest a ferromagnetic correlation in system enhanced by oxygen content. In addition, a low temperature thermal activation resistivity induced by fields was observed in single crystals annealed in oxygen atmosphere.

PACS numbers: 75.47.-m, 71.30.+h, 75.30.Fv, 75.50.Gg

I. INTRODUCTION

Misfit-layered cobalt oxides attracted a great deal of interest for their possession of unusual electrical properties such as large negative magnetoresistance,^{1,2,3,4} coherent-incoherent transition with varying temperature in $(\text{Bi,Pb})_2\text{Ba}_3\text{Co}_2\text{O}_9$,⁵ and a large thermoelectric power (TP) with metallic resistivity observed in $(\text{Bi,Pb})_2\text{Sr}_2\text{Co}_2\text{O}_9$,^{5,6} $\text{Ca}_3\text{Co}_4\text{O}_9$ ($[\text{Ca}_2\text{CoO}_{3-\delta}]_{0.62}[\text{CoO}_2]$),¹ and $\text{Tl}_{0.4}(\text{Sr}_{0.9}\text{O})_{1.12}\text{CoO}_2$.⁷ Besides the effort to enhance the thermoelectric figure of merit $ZT=S^2T/\rho\kappa$ for the application reason, as a transition metal oxide with strong correlation and anomalous electronic structure, many studies were focused on their physical nature. Recently, another promising thermoelectric triangular cobaltite Na_xCoO_2 , was found to exhibit superconductivity below 5 K by intercalating water molecules into between the Na^+ and CoO_2 layers in the composition of $x=0.35$.⁸ Later, Foo et al.⁹ observed an insulating resistivity below 50 K in the composition of $x=0.5$, which is related to the strong coupling of the holes and the long-range ordered Na^+ ions. The strong dependence of thermopower on magnetic field in Na_xCoO_2 provides a unambiguous evidence of strong electron-electron correlation in the thermoelectric cobalt oxides.¹⁰ The large TP with metallic resistivity, superconductivity, charge ordering existing in various x , displays a complicated and profuse electronic state in Na_xCoO_2 . This has inspired numerous theoretical and experimental studies on the thermoelectric cobaltite.

In this paper we focus on one of the thermoelectric cobalt oxides, $[\text{Ca}_2\text{CoO}_{3-\delta}]_{0.62}[\text{CoO}_2]$ system. Because of the large ZT (~ 1 at 1000 K),¹¹ $\text{Ca}_3\text{Co}_4\text{O}_9$ is thought to be one of the most promising candidate for a p-type material component of thermoelectric power generation systems. $[\text{Ca}_2\text{CoO}_{3-\delta}]_{0.62}[\text{CoO}_2]$ has a complex magnetic structure, including the spin-state transition of cobalt ions from low-spin to intermediate-spin+high-spin or high-spin at about 380 K, the spin density wave transition with onset temperature $T_{\text{SDW}}^{\text{on}}=100$ K and tran-

sition width $\Delta T=70$ K, and the ferrimagnetism below 19 K.^{1,12} Transport properties are closely related to the magnetism due to the coupling between the charge and spin degree of freedom. The spin state transition of cobalt ions around 380 K leads to an abrupt jump of resistivity with decreasing temperature;^{1,12} the emergence of insulator-like behavior below about 70 K was thought to be related to the appearance of short-range SDW order.¹² $[\text{Ca}_2\text{CoO}_{3-\delta}]_{0.62}[\text{CoO}_2]$ also has a complex crystal structure. The crystal structure of $[\text{Ca}_2\text{CoO}_{3-\delta}]_{0.62}[\text{CoO}_2]$ consists of alternating stacks of two monoclinic subsystems along the c-axis: the triple $\text{Ca}_2\text{CoO}_{3+\delta}$ rocksalt-type layers and single CdI_2 -type CoO_2 triangular sheet (conducting layers).¹ The misfit between the two subsystems leads to an incommensurate (IC) spatial modulation along b axis. The $[\text{Ca}_2\text{CoO}_{3-\delta}]_{0.62}[\text{CoO}_2]$ system could exhibit very complicated electronic transport properties due to the complex magnetic and crystal structure. Strong magnetic field is a very useful tool to investigate the correlation between charge dynamics and magnetism. The interesting phenomenon could be expected under high magnetic field due to the strong coupling between the charge and spin degrees of freedom. Large negative MR has been reported in previous work,¹ but only on curve of $\rho(T)$ vs. T under the magnetic field of 7 T was presented. Detailed investigation is lacking to make out the mechanism for the MR yet. In this paper, the $\rho_{ab}(T)$ is studied with varying annealing condition. It is found that the $\rho_{ab}(T)$ exhibits a minimum. The temperature corresponding to this minimum (T_{min}) increases with the loss of oxygen content, indicative of the enhancement of SDW. The magnetoresistance were also measured up to 14 T in the $[\text{Ca}_2\text{CoO}_{3-\delta}]_{0.62}[\text{CoO}_2]$ single crystals. Large negative MR was observed in all samples. An insulator-to-metal (IM) transition were observed for oxygen annealed crystals in high magnetic fields. The magnetic-field-driven charge dynamics is attributed to the enhancement of ferromagnetic correlation.

II. EXPERIMENTAL

The single crystals used in the measurements were grown by the solution method as described in ref.(13) using K_2CO_3 -KCl as fluxes with composition of 4:1. The typical dimension of the crystals are $5 \times 5 \times 0.02$ mm³. In order to study the oxygen content (or carrier concentration) effect on the charge transport, as-grown crystals were annealed in flowing oxygen atmosphere at 723 K for 12 h, 11 h, 10 h and 8 h, which were denoted as crystal A, B, C and D, respectively. The as-grown crystal is denoted as crystal E. Some other crystals were annealed in flowing nitrogen atmosphere at 723 K for 10 h, denoted as crystal F. We found that the charge transport is sensitive to the annealing time (oxygen content). The details will be discussed in the following section. This result is consistent with the reported by Karppinen et al.¹⁴ Resistance measurements were performed using the ac four-probe method with an ac resistance bridge system (Linear Research, Inc.; LR-700P). The dc magnetic field for magnetoresistance measurements is supplied by a superconducting magnet system (Oxford Instruments). In the text following, we abbreviate $[Ca_2CoO_{3-\delta}]_{0.62}[CoO_2]$ to $Ca_3Co_4O_9$ for simplicity.

III. EXPERIMENTAL RESULTS

A. Transport properties

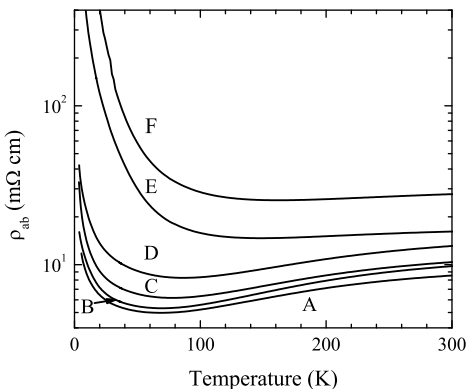


FIG. 1: The temperature dependence of resistivity for the $Ca_3Co_4O_9$ crystals annealed in various conditions. The curve A, B, C, D correspond to the resistivity of the crystal annealed in oxygen flow at 723 K for 12 h, 11h, 10h, 8h, respectively. The curve E and F are obtained from as-grown crystal and nitrogen-annealed crystal, respectively.

Figure 1 shows the $\rho(T)$ curves of the $Ca_3Co_4O_9$ single crystals annealed in various conditions. There are some common features in $\rho(T)$ among the crystals. The $\rho(T)$ is metallic in high temperatures and shows a broad minimum with decreasing temperature. Below the temperature of resistivity minimum (T_{\min}), the $\rho(T)$ exhibits a diverging behavior. The crystal A, which was annealed in oxygen flow at 723 K for 12 h has the lowest resis-

tivity (the curve A) and T_{\min} (68.8 K) among the listed samples. The ratio $\rho(T=4 \text{ K})/\rho(T=300 \text{ K})$ is also the smallest. This indicates that this sample corresponds to the highest hole concentration. With decreasing the annealing time in oxygen flow at 723 K, T_{\min} and the ratio $\rho(T=4 \text{ K})/\rho(T=300 \text{ K})$ increases, indicative of the decrease of the hole concentration. This demonstrates that annealing in oxygen atmosphere enhances the oxygen content in the crystals. The hole concentration increases with the enhancement of oxygen content. The crystal annealed in nitrogen flow exhibits the largest resistivity among all samples, and it also possesses the largest T_{\min} (~ 169 K), indicating that this crystal have the lowest hole concentrations and oxygen content. The as-grown crystal has the resistivity and T_{\min} between that of the oxygen-annealed crystals and nitrogen-annealed one, manifesting a hole concentration between them. Thus the annealing in nitrogen flow is a procedure of reducing oxygen content, while in oxygen flow enhancing oxygen content. This is consistent with the results reported by Karppinen et al.¹⁴ They found that the oxygen content is easily changed just by ambient pressure in low oxygen content regime. The δ difference in $Ca_3Co_4O_{9+\delta}$ is as high as 0.24 between N_2 annealed sample and sample prepared in air. However, the annealing has to be performed at high oxygen pressure to change the oxygen content in the large δ regime. The difference between our and their works is that their work was carried out on the polycrystalline samples, while the data presented here on single crystals. Fig. 1 clearly shows that the charge transport is sensitive to the oxygen content in the crystals, which increases with enhancing annealing time at 723 K in oxygen flow. In addition, it can be found that T_{\min} decreases with increasing the oxygen content from 149 K in the curve E to 68.8 K in the curve A. Sugiyama et al. suggested that the resistivity minimum is associated with the SDW transition. According to this point of view, the SDW can be enhanced by decreasing the oxygen content, equivalently, reducing the Co ions valence. This is consistent with the effect of Bi and Y doping in the $Ca_3Co_4O_9$, where the T_{SDW}^{on} is enhanced by 30 K at the doping level of 0.3 with decreasing the Co valence. These results indicate that the SDW is very sensitive to the Co ions valence. It should be pointed out that annealing in nitrogen may have a much stronger effect on the enhancement of SDW than the Y and Bi doping because the T_{\min} of the curve F is enhanced by about 100 K relative to that of curve A, though the exact transition temperature of SDW cannot be determined.

B. Magnetotransport phenomena

1. Magnetoresistance

Figure 2(a) shows the in-plane resistivity of the crystal A as the function of temperature in the range of 4 K to 70 K in various magnetic fields up to 14 T. This crystal was annealed in oxygen flow at 723 K for 12 h. The

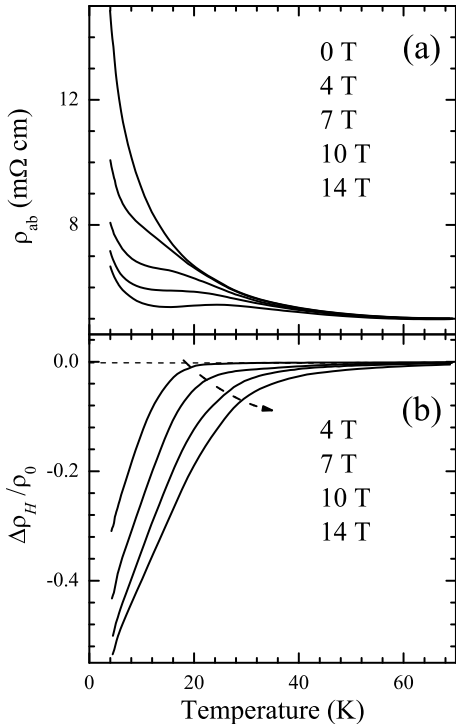


FIG. 2: (a) The temperature dependence of the resistivity for the crystal A at different fields. (b) The temperature dependence of $\Delta\rho_H/\rho_0 = [\rho(H) - \rho(0)]/\rho(0)$ at different fields. The dashed arrow in the (b) guides one's eyes for the temperature below which the negative MR begins to increase rapidly.

field is applied along the c -axis. At zero field the sample is metallic ($d\rho_{ab}/dT > 0$) in high temperatures, and exhibits a minimum of $\rho(T)$ at 68.8 K. Below 68.8 K the crystal shows an insulator-like behavior. The $\rho(T)$ in whole range of T at zero field has been shown by the curve A of fig. 1. The value of $\rho_{ab}(T)$ is suppressed strongly at low temperature by magnetic field, with MR $[=(\rho(T, H) - \rho(T, 0))/\rho(T, 0)]$ reaching -55% at 4 K and 14 T. The large negative MR comes from the reduction of spin scattering, which reflects a spin polarized transport. The reduction of spin scattering originates from the ferromagnetic correlation, which can be deduced from the ferrimagnetic transition at about 19 K. The negative MR shown in fig. 2(b) increases with decreasing the temperature, in contrast to the CMR in manganites¹⁵ or $\text{ReBaCo}_2\text{O}_{5+\delta}$,^{16,17} in which a maximum of MR can be observed around the phase transition temperature. This indicates that the ferromagnetic correlation in the conducting layers is rather weak or some fluctuation exists in the system. Figure 2(b) shows a large negative MR below 20 K at 4 T, but no obvious MR above 20 K. This temperature is almost the same as that of the ferrimagnetic transition, reflecting the close relation between the spin polarized transport and the ferromagnetic correlation inferred from ferrimagnetism. The MR displayed in fig. 2(b) increases abruptly below a certain temperature at different fields (as indexed by the dashed arrow), and

this temperature increases with enhancing external magnetic field. Such a temperature should correspond to the ferrimagnetic transition, which would be enhanced with increasing magnetic field. These results support that the large negative MR arises from the ferromagnetic correlation in conducting layers.

2. Magnetic-field-induced IM transition

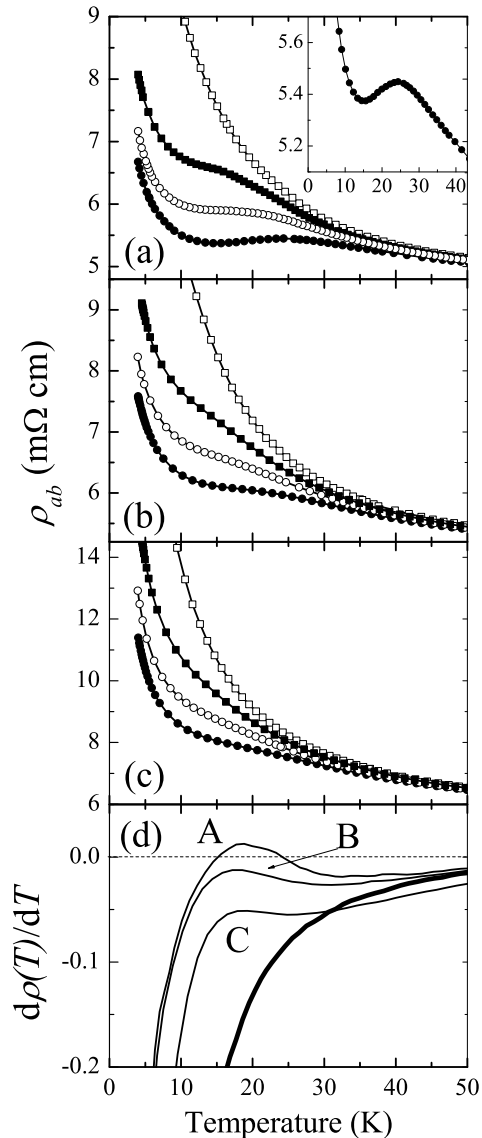


FIG. 3: Magneto-resistivity of the crystal A (a), B (b) and C (c) plotted against T in detail at magnetic fields of 0 T (\square), 7 T (\blacksquare), 10 T (\circ) and 14 T (\bullet), respectively. (d) The slope of $\rho(T)$ under the field of 14 T for crystal A, B and C (solid lines) and of $\rho(T)$ without field (bold line) for crystal A plotted against T . The inset shows the magnified plot of 14 T data of crystal A in order to exhibit the IM transition clearly.

A most intriguing result in fig. 2(a) is that a field-induced weak insulator-to-metal transition at 14 T can be

observed at about 25 K. The data below 50 K at 0, 7, 10, 14 T for crystal A, B, C are plotted in the fig. 3(a), (b), and (c), respectively. In fig. 3(a), there exhibits a clear downturn of $\rho(T)$ at about 25 K for 14 T data, at which the sign of slope $d\rho(T)/dT$ is changed from negative to positive, indicating that an insulator-metal transition is induced by magnetic field. Compared to the zero field curve, $\rho(T)$ in magnetic fields lower than 14 T shows a notable change of the slope ($d\rho(T)/dT$) at low temperature. Fig. 3(a) shows that even $\rho(T)$ at 4 T begins to possess the marked change of the slope. It is similar to the cusp structure of $\rho(T)$ of $\text{Bi}_{2-x}\text{Pb}_x\text{Sr}_2\text{Co}_2\text{O}_y$ single crystals with $x=0.51$. In $\text{Bi}_{2-x}\text{Pb}_x\text{Sr}_2\text{Co}_2\text{O}_y$ single crystals, the zero field $\rho(T)$ shows an obvious downturn at 5 K for $x=0.51$, which is thought to correspond to the ferromagnetic transition.⁴ The cusp shifts to higher temperature with increasing magnetic field. This is also similar to the rapidly downturn of $\rho(T)$ around ferromagnetic transition with decreasing T in the perovskite manganites¹⁵ and cobalt oxides¹⁸. These suggest that the $\text{Ca}_3\text{Co}_4\text{O}_9$ system is close to ferromagnetic transition, especially in high magnetic field, though a ferromagnetic transition has not been found in this system experimentally yet. In the crystal A, ferrimagnetism instead of ferromagnetism was observed in weak magnetic field. No measurement has been performed in high field. Nonetheless, inferred from the a notable change of the slope of $\rho(T)$ in magnetic field, our results seem to suggest that ferrimagnetism to ferromagnetism transition possibly occurs when magnetic field is enhanced.

For the crystal B and C with less oxygen content relative to the crystal A, no downturn behavior in $\rho(T)$ is observed even at 14 T, but it shows a remarkable change in the slope $d\rho/dT$ at the ferrimagnetic transition temperature (T_{FR}), as shown in fig. 3(b) and 3(c). In order to show clearly the above behavior, the slope $d\rho/dT$ vs. T curve presented in Fig. 3(d). The $d\rho(T)/dT$ at zero field varies monotonically with temperature, while $d\rho(T)/dT$ at 14 T for these three samples show a clear dip-hump structure, which reveals a noticeable change of the slope of $\rho(T)$ around 10 K-30 K in magnetic field. The increase of the $d\rho(T)/dT$ toward to positive value with decreasing T indicates a downturn tendency of $\rho(T)$. Obviously, the tendency of the downturn of $\rho(T)$ decreases with reducing the oxygen content. A positive $d\rho/dT$ is clearly shown in fig. 3(d) for the crystal A at 14 T, indicative of an insulator-metal transition. The field-induced IM transition is ascribed to the enhancement of ferromagnetic correlation. Thus the ferromagnetic correlation is reduced with the loss of oxygen content. As shown in fig. 1, SDW order is enhanced by the reduction of oxygen content. Thus the ferromagnetic correlation seems to be *competing* with the SDW.

3. Magnetotransport in the as-grown crystal

Compared to crystal A-D, the as-grown crystal E has a lower carrier concentration and thus a higher resistivity.

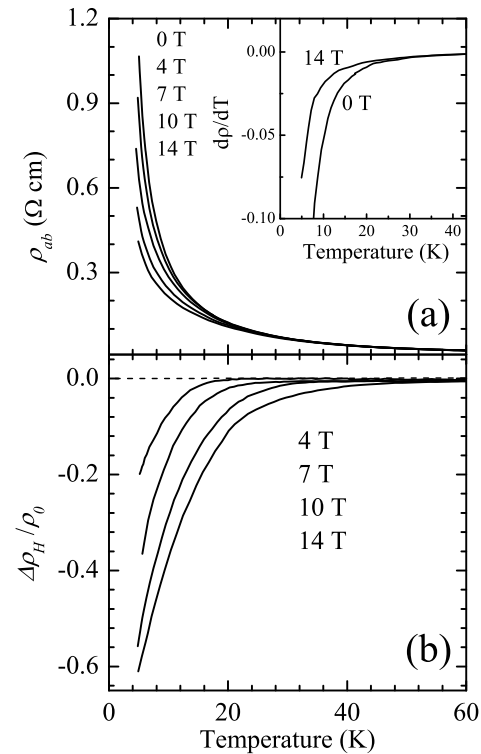


FIG. 4: (a) The temperature dependence of the transverse magnetoresistivity the in as-grown crystal. (b) Temperature dependence of the MR in various fields.

Figure 4(a) shows the magnetoresistivity for the as-grown crystal at various magnetic fields. The large negative MR is also observed at low temperature, like the crystal A-D. While no sign for a field-driven IM transition can be found even at 14 T (see the inset of fig. 4(a)). A reduction of carrier concentration in the as-grown crystal relative to the oxygen annealed ones could lead to an enhancement of SDW order as in the Bi- or Y-for-Ca substitution in $\text{Ca}_3\text{Co}_4\text{O}_{9+\delta}$ samples.¹² In the literature, it is reported that the SDW transition temperature is increased by ~ 30 K due to either Bi or Y doping with $x=0.3$ in $\text{Ca}_{3-x}\text{M}_x\text{Co}_4\text{O}_9$ ($\text{M}=\text{Bi}, \text{Y}$). The T_{min} for the as-grown crystal at zero field is 149 K, which is much higher than that observed in the crystals annealed in oxygen flow. T_{min} is associated to the SDW order.¹² Thus the increase of T_{min} is consistent with the enhancement of the SDW due to reduction of carrier concentration. In fig. 4(b), the $\Delta\rho_H/\rho_0$ shows negative value, indicative of a spin polarized transport like in crystal A. One can notice that in fig. 4(b) the temperature for the $\Delta\rho_H/\rho_0$ beginning to show negative value enhances with increasing magnetic field, suggesting a enhancement of ferromagnetic correlation with increasing magnetic field as in crystal A. Nonetheless, the ferromagnetic correlation is much weaker than that in the crystals annealed in oxygen so that no sign of downturn tendency of $\rho(T)$ can be found at 14 T in spite of the large negative MR. While a larger negative MR relative to crystal A is observed at

14 T in crystal E. The possible reason for this result will be discussed in the following.

4. *The effect of annealing condition on the transport behavior*

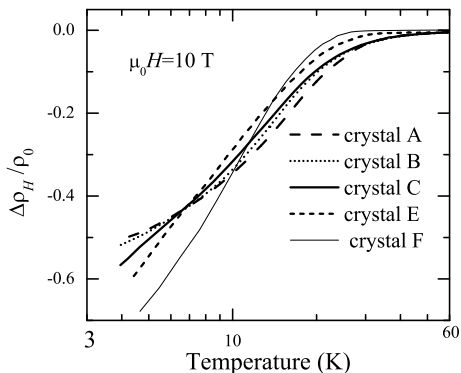


FIG. 5: The magnetoresistance at 10 T as a function of T in the crystal A-C, E, and F.

According to the results above, the annealing condition affects the transport and magnetotransport behaviors strongly. Obviously, the transport behavior is changed by varying oxygen content, i.e. by varying the Co ions valence. From crystal A to F, the evolution of resistivity indicates that the hole concentration is reduced due to the loss of oxygen content. The reduction of the Co ions valence due to the loss of oxygen content enhances the SDW order dramatically, which can be inferred from the large increase of the T_{\min} as discussed above. Spin density wave is basically antiferromagnetic, thus one can conclude that there is antiferromagnetic correlation in the system and the loss of the oxygen favors the enhancement of the antiferromagnetic correlation. Nonetheless, the ferrimagnetism and the large negative MR in the crystals suggest that there also exists ferromagnetic correlation. Figure 5 exhibits the $\Delta\rho(H = 10\text{T})/\rho(H = 0\text{T})$ vs. T for crystals A-C, E, and F, respectively. Clearly, the temperature below which the negative MR is observable increases with enhancing oxygen content. At very low temperature, the absolute value of $\Delta\rho_H/\rho_0$ increases with reducing the oxygen content. With increasing T , it gradually evolves to a completely opposite variation with oxygen content, that is, the absolute value of $\Delta\rho_H/\rho_0$ decreases with reducing the oxygen content. This is very similar to the evolution of $\Delta\rho_H/\rho_0$ with lead doping level in $(\text{Bi,Pb})_2\text{Sr}_2\text{Co}_2\text{O}_y$ system (Ref. 4, fig. 9). With increasing Pb doping level, the temperature below which negative MR is observable increases, and the value of MR is enhanced in the temperature range from 8 to 40 K, while reduced below 8 K.⁴ In $(\text{Bi,Pb})_2\text{Sr}_2\text{Co}_2\text{O}_y$, the increase of hole concentration due to Pb doping leads to a transition from paramagnetism in Pb-free sample to weak ferromagnetism in the sample with $\text{Pb}=0.51$.⁴ Thus the

fig. 5 suggests that the enhancement of oxygen content, i.e. the increase of Co ions valence, leads to the increase of the ferromagnetic spin correlation. This is consistent with conclusion inferred from the evolution of the field-induced IM transition by comparing the fig. 3 and fig. 4.

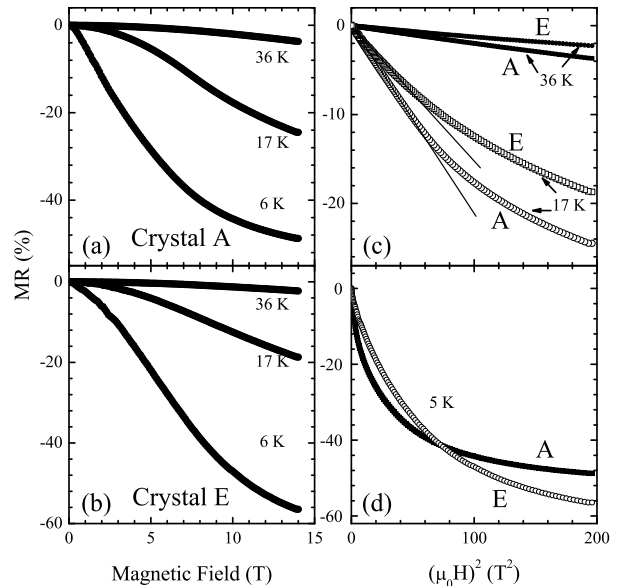


FIG. 6: The isothermal magnetoresistance as a function of magnetic field for crystal A (a) and E (b), respectively. The same data are replotted in (c) and (d) in the square magnetic field scale.

The isothermal MR shown in fig. 6(a) and 6(b) further confirms this speculation. Fig. 6(a) and 6(b) shows the isothermal MR for the crystal A and E, respectively. At 36 K and 17 K, the MR is larger in crystal A. While at 6 K, the MR in crystal A is smaller than that in crystal E below about 8.5 T, and with further increasing magnetic field, the MR in crystal A becomes the smaller one (also see fig. 6(d)). At 36 K and 17 K, the MR shows no saturation tendency, indicating that the spins is far from being completely polarized. The larger MR value in crystal A at 36 K and 17 K suggests a more polarized transport and thus a stronger ferromagnetic correlation. At 6 K, there is a clear saturation tendency of MR in high magnetic field in both crystals. The larger MR in lower field in crystal A indicates that the spin in this sample is easier to be polarized, since the magnetotransport is thought to be a spin polarized transport. The saturation of MR suggests a tendency of completely polarized spins. The smaller MR in crystal A at 6 K in high magnetic field suggests a less spin disordered transport. All of these strongly suggest a stronger ferromagnetic correlation in crystal A and definitely support the speculation that the enhancement of oxygen content leads to the increase of the ferromagnetic spin correlation.

Fig. 6(a) and 6(b) is replotted in fig. 6(c) and 6(d) in square magnetic field scale. At 36 K, it is found that the

MR of the two crystals is proportional to H^2 . While the MR at 17 K is proportional to H^2 only in low magnetic fields and deviates from H^2 law in high magnetic fields. At the lower T , 6 K, it disobeys H^2 law from zero field. These results suggest that there are probably different mechanisms for the negative MR at high T and low T . It should be pointed out that at 36 K there is (short-range) IC-SDW order only, while 6 K is far below the ferrimagnetic transition, at which the the ferrimagnetism and (long-range) IC-SDW order coexist. consequently, the MR at 36 K only can reflect the property related to SDW state. While the MR at 6 K should mostly reveal the effect of ferrimagnetism. 17 K is just below the ferrimagnetic transition, thus the MR at this temperature involves the influence of these two magnetisms.

5. The influence of oxygen content and magnetic field on the SDW order

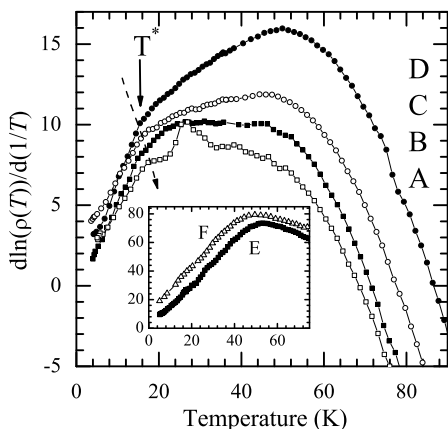


FIG. 7: Logarithmic derivatives of the zero-field resistivity vs. T for crystal A, B, C, and D respectively. The inset shows the T dependence of the Logarithmic derivatives of the zero-field resistivity of crystal E.

Why negative MR can be observed in IC-SDW state? In previous SDW materials, such as organic conductors $(\text{TMTSF})_2\text{X}$ (TMTSF : Tetramethyltetraselena-fulvalene, $\text{X}=\text{PF}_6, \text{NO}_3$ and ClO_4),^{19,20,21} were reported to show positive MR in SDW state. In order to investigate the nature of such negative MR, the effect of a magnetic field on the SDW order should be performed. Usually, in a SDW state, the resistivity $\rho(T)$ can be expressed as^{12,23}

$$\frac{1}{\rho} = \mu(T) \exp\left(-\frac{\Delta_g}{k_B T}\right), \quad (1)$$

where $\mu(T)$ is the mobility of carriers, Δ_g is the gap energy, and k_B is the Boltzmann constant. Usually, $\mu(T)$ is independent of T . Using Eq. (1), the $\rho(T)$ of crystals A-D in T between 50 and 20-30 K can be fitted by assuming that $\mu(T)$ is independent of T . In this case, $\text{dln}\rho/\text{d}(1/T)$ can be calculated to reflect the activation energy, Δ_g .²²

Fig. 7 shows the $\text{dln}\rho/\text{d}(1/T)$ plotted against T for all the crystals. Plateaus are observed in crystals A-D in the T ranging from 20-50 K. This reveals that in these samples there are T independent gap within this temperature range, which could be opened by SDW. Fig. 7 exhibits that the value of the plateau of $\text{dln}\rho/\text{d}(1/T)$ increases from crystal A to D. This is consistent with the evolution of T_{min} with the oxygen content, which reflects the SDW is enhanced by decreasing oxygen content. Thus it may suggest that the observed energy gap is opened by SDW.²³ According to μSR and $\mu^+\text{SR}$ results,¹² it is considered that a short-range order IC-SDW state appears below 100 K, while the long-range order is completed below 30 K. In fig. 7, $\text{dln}\rho/\text{d}(1/T)$ varies smoothly through 30 K with decreasing temperature, except for the crystal A. In crystal A, a sharp peak is observed around 27 K. The susceptibility and $\mu^+\text{SR}$ experiment reveal that the long-range SDW order completes at this temperature.¹² Moreover, the sharp peak of $\text{dln}\rho/\text{d}(1/T)$ was thought to correspond to the SDW transition temperature.^{19,20,21} Thus, the peak of $\text{dln}\rho/\text{d}(1/T)$ in crystal A corresponds to the temperature where long-range SDW order completes. Even so, the value of $\text{dln}\rho/\text{d}(1/T)$ is almost the same at the two sides of the peak. Fig. 7 indicates that the influence of short-range and long-range IC-SDW order in this sample on the transport properties is the same.

The Eq. (1) cannot be applied in the whole range of T below 50 K because the $\text{dln}\rho/\text{d}(1/T)$ shows a rapidly decrease below a temperature around 20 K, which is indexed as T^* in fig. 7. According to the susceptibility experiment,¹² a ferrimagnetic transition occurs around this temperature. This suggests that the abrupt decrease of $\text{dln}\rho/\text{d}(1/T)$ below T^* arises from the ferrimagnetic transition. With increasing oxygen content from crystal D to crystal A, the T^* enhances slightly. The $\text{dln}\rho/\text{d}(1/T)$ reflects the activation gap. Thus, the abrupt drop of $\text{dln}\rho/\text{d}(1/T)$ suggests that the ferrimagnetic transition reduces or hides the SDW gap. The inset shows the $\text{dln}\rho/\text{d}(1/T)$ of crystal E and F. In this two samples no plateau is observed, suggesting Eq. (1) is not feasible any more or the $\mu(T)$ is dependent on T in this two samples. There is no anomaly below 20 K, which could be due to the stronger SDW order and rather weaker ferrimagnetism in these two samples relative to the crystals annealed in oxygen atmosphere. The effect of ferrimagnetism is hidden by the strong SDW order.

In order to study the influence of magnetic field on the SDW state, the $\text{dln}\rho/\text{d}(1/T)$ as a function of T at various magnetic field in the two samples is shown in Fig. 8(a). It is observed that the value of the plateau decreases with increasing field, indicating the reduction of the activation gap. While above 50 K, the $\text{dln}\rho/\text{d}(1/T)$ is almost independent of magnetic field. As discussed above, the gap opening can be ascribed to the SDW order. If so, it suggests that the SDW order here is suppressed by magnetic field. The peak around 27 K disappears when field is as high as 7 T, suggesting that the SDW is suppressed indeed. This can be used to explain

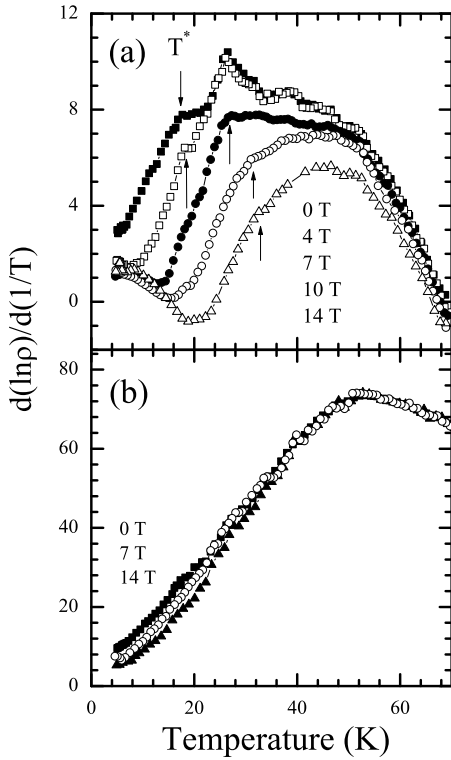


FIG. 8: (a) The logarithmic derivative of the resistivity of crystal A as a function of the temperature at 0, 4, 7, 10, and 14 T. (b) The temperature dependence of The logarithmic derivative of the resistivity of crystal E at 0, 7, 14 T.

the negative MR far above the ferrimagnetic transition temperature, which has a different H dependence of the MR from that in ferrimagnetic state. Since the upturn resistivity below T_{\min} is associated with the SDW order, a suppression of SDW certainly leads to negative MR. In fig. 8(a), T^* increases with increasing magnetic field, while the slope of the $\ln\rho/d(1/T)$ remains unchanged below T^* . The enhancement of the T^* is related to the increase of ferrimagnetic transition temperature in magnetic field, consistent with the MR data in Fig. 2(b). Clearly, *the ferrimagnetic ground state is competing with the SDW ground state*. The suppression of SDW in high magnetic field may be related to the enhancement of the ferromagnetic correlation. Another triangular layered cobaltite should be mentioned to compare with $[\text{Ca}_2\text{CoO}_3]_{0.62}[\text{CoO}_2]$ is Na_xCoO_2 . In $\text{Na}_{0.75}\text{CoO}_2$, SDW and weakly ferromagnetism coexist,^{24,25,26} while a large positive MR was observed in magnetic state,²⁷ contrasting to the negative MR in $[\text{Ca}_2\text{CoO}_3]_{0.62}[\text{CoO}_2]$. The negative MR in $[\text{Ca}_2\text{CoO}_3]_{0.62}[\text{CoO}_2]$ originates from the reduction of the spin scattering of carriers, while in $\text{Na}_{0.75}\text{CoO}_2$, the MR seems to be more possible coming from the change of carrier-mobility in Fermi surfaces in magnetic field due to a pseudogap formation.²⁷ In spite of the weakly ferromagnetism, the pseudogap formation leads to a positive MR in the $\text{Na}_{0.75}\text{CoO}_2$. Finally, we note that the $\ln\rho/d(1/T)$ vs. T curve in fig.

8(b) for crystal E remains unchanged above 20 K with varying magnetic field, suggesting that the SDW is too strong to be suppressed by magnetic field. Below 20 K, the $\ln\rho/d(1/T)$ decreases with increasing magnetic field, manifesting that there still is ferrimagnetic transition in crystal E in spite of the reduction of oxygen content with respect to the crystal A. This further demonstrates the point of view that the ferromagnetic correlation leads to the large negative MR.

C. Thermal-activation transport in magnetic field at low temperature

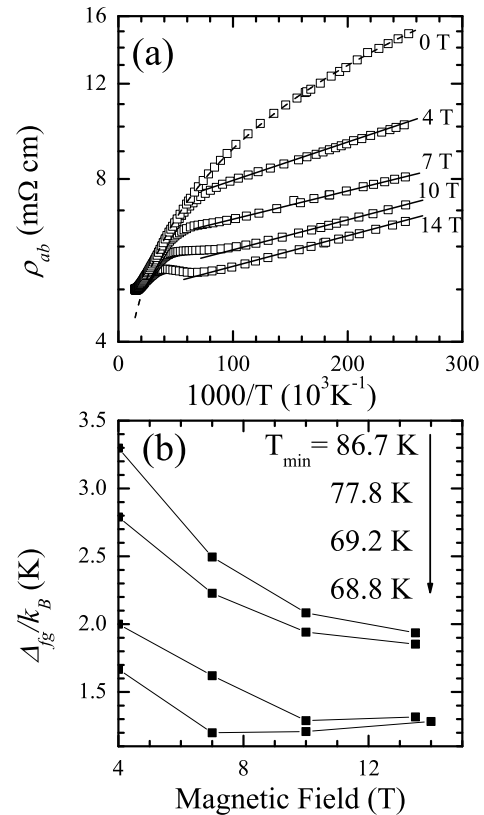


FIG. 9: (a) Arrhenius plot for the data of fig. 1(a). The dashed line is the fitting data with Mott variable range hopping law. The solid line is the fit data with the thermal activation formalism. (b) The field-induced energy gap (Δ_{fg}) plotted against magnetic field for four crystals with different T_{\min} .

In Fig. 8(a) another intriguing feature can be found in the low temperature range, the $\ln\rho/d(1/T)$ shows a T -independent behavior below about 10 K for the data in magnetic field. It suggests that there is another thermal activation transport. The Arrhenius plot of the data in fig. 1(a) is displayed in fig. 9(a), which clearly shows that the temperature dependence of the resistivity under different fields exhibits an Arrhenius-type behavior below about 12 K, that is, $\rho(T) \propto e^{\Delta/k_B T}$, where Δ is gap energy and k_B is Boltzmann constant. It suggests that

the resistivity in low temperature range under the fields follows the thermal activation model. While the zero field data below 30 K can be well fitted by a formula $\rho(T) = Ae^{(T_0/T)^{1/4}}$, indicative of Mott variable range hopping (VRH) law. It implies that an energy gap is opened by magnetic field. It should be pointed out that this phenomenon was observed in all of the four oxygen annealed crystals A-D, with different T_{\min} . The obtained gap energy depends on T_{\min} . Figure 9(b) shows the magnetic dependence of the field-induced gap energy for the four crystals. It is found that the gap energy increases with increasing T_{\min} . While it decreases with increasing magnetic fields, and saturates in high field. It should be pointed out that no such phenomenon is observed in the as-grown crystal and the sample annealed in N_2 . The nature of this field-induced thermal activation transport is not well understood yet. The gap energy shown in fig. 9(b) is dependent on T_{\min} , suggesting that the gap may be associated with the SDW order.

IV. DISCUSSION

Large negative MR has been observed in many misfit-layered cobaltites, such as: $(Bi, Pb)_2Sr_2Co_2O_y$, $[Sr_{1.9}Pb_{0.7}Co_{0.4}O_3][CoO_2]_{1.8}$, $[Bi_{1.7}Co_{0.3}Ca_2O_4][CoO_2]_{1.67}$, and $[Ca_2CoO_{3-\delta}]_{0.62}[CoO_2]$ studied in this paper. In some of these cobaltites, such as $[Sr_{1.9}Pb_{0.7}Co_{0.4}O_3][CoO_2]_{1.8}$ and $[Bi_{1.7}Co_{0.3}Ca_2O_4][CoO_2]_{1.67}$, spin density wave was observed.²⁵ While in some others, like $(Bi, Pb)_2Sr_2Co_2O_y$, ferromagnetic transition was observed. In $[Ca_2CoO_{3-\delta}]_{0.62}[CoO_2]$ single crystals, spin density wave and ferrimagnetic transition were observed by μ^+ SR and susceptibility experiments,¹² respectively.

Na_xCoO_2 is the most extensively studied at experimental and theoretical level in the layered cobaltites with triangular $[CoO_2]$ layers as basic structure units. Because of the very similar structure of $[CoO_2]$ layers, most of the results obtained in Na_xCoO_2 can be reproduced in the misfit cobaltites. The low-spin state of Co^{3+} and Co^{4+} predicted by Singh in Na_xCoO_2 ,²⁸ is found to hold in $(Bi, Pb)_2Sr_2Co_2O_y$ by photoemission experiment.³⁰ Another prediction by Singh in Na_xCoO_2 , that the t_{2g} orbitals are split into a_{1g} and e'_g subbands due to rhombohedral crystal field,²⁸ is feasible in $(Bi, Pb)_2Sr_2Co_2O_y$. Obviously, some theoretical results obtained in Na_xCoO_2 can be used in the misfit cobaltites.

A very important prediction from local spin density approximation (LSDA) band calculation by Singh is the ferromagnetic instability in Na_xCoO_2 .^{28,29} While experimentally, ferromagnetism has not been observed. Only weakly ferromagnetism^{24,25,26} or metamagnetism³¹ was observed, which is probably due to quantum fluctuation.^{24,28,29} Neutron inelastic scattering gives evidences for the existence of ferromagnetic (FM) spin fluctuation within the $[CoO_2]$ layers in $Na_{0.75}CoO_2$ single crystal.²⁴ The weak ferromagnetism in $Na_{0.75}CoO_2$ was thought to originate from a canted-SDW^{25,26} or a spin

arrangement with an in-plane ferromagnetic order and a SDW modulation perpendicular to the planes.²⁴ Metamagnetism in $Na_{0.85}CoO_2$ was suggested to favor the in-plane ferromagnetic correlation and interplane anti-ferromagnetic (AF) coupling.³¹ The Metamagnetism was thought to be a spin-flop transition from an AF to a FM state along c-axis.³¹ The ferromagnetic spin correlation is very sensitive to the Co ions valence in the triangular cobaltites. In $(Bi, Pb)_2Sr_2Co_2O_y$,⁴ with increasing Pb doping level from zero to 0.51, it can change from paramagnetism to weak ferromagnetism. Though no ferromagnetism is observed in $[Ca_2CoO_{3-\delta}]_{0.62}[CoO_2]$, it shows similar MR behavior to $(Bi, Pb)_2Sr_2Co_2O_y$, especially the variation of the MR with oxygen content in fig. 5 is very similar to the evolution of MR with Pb doping level in $(Bi, Pb)_2Sr_2Co_2O_y$. In the $[Ca_2CoO_{3-\delta}]_{0.62}[CoO_2]$ crystals, a ferrimagnetism was found below 19 K in susceptibility experiment, suggesting the ferromagnetic correlation in conducting CoO_2 layers safely. The evolution of MR with oxygen content and the field-induced downturn of $\rho(T)$ indicate that the ferromagnetic correlation varies dramatically with Co ions valence. Especially, the field-induced IM transition in crystal A occurs at the ferrimagnetic transition. This is similar to the insulator-metal transition induced by field at the ferromagnetic transition in $(Bi, Pb)_2Sr_2Co_2O_y$ with $Pb=0.51$.⁴ The $Na_{0.75}CoO_2$, which possesses weak ferromagnetism,^{24,25,26,27,31} exhibits large positive instead of negative MR observed in $(Bi, Pb)_2Sr_2Co_2O_y$. This was considered to be due to a pseudogap formation deduced from the abrupt downturn of resistivity.²⁷

Another interesting magnetic property in this system is spin density wave. The SDW emerges from much higher temperature than ferrimagnetism.¹² According to our data, the negative MR appears far below T_{\min} , and it coincides with the ferrimagnetic transition. In contrast to ferromagnetic correlation, the SDW has a complete opposite response to Co ion valence. The SDW enhances with reducing Co ion valence according to the change of T_{\min} . This indicates that the ferrimagnetism and the SDW order are *competing*.

It is worthy of note that the SDW and ferromagnetic correlation affect the transport and magnetotransport properties strongly, suggesting that the SDW and ferromagnetic correlation coexist in the $[CoO_2]$ conducting sheets below ferrimagnetic transition temperature. The μ^+ SR experiments have suggested the coexistence of the IC-SDW state and ferrimagnetism below 19 K.¹² Sugiyama et al. suggested that the two subsystems of the crystal structure (the $[Ca_2CoO_{3-\delta}]$ rocksalt-type layers and the $[CoO_2]$ triangular sheets) act directly as the two magnetic sublattices for the ferrimagnetism.¹² From this picture, one can naturally infer the existence of ferromagnetic spin arrangement in the $[CoO_2]$ sheets. Large negative MR and the field-induced IM transition seems to support this picture for the ferromagnetic correlation in the conducting $[CoO_2]$ sheets. However, we cannot give detailed picture how the spin arrangement for the

coexistence of ferrimagnetism and the (long-range order) IC-SDW below T_{FR} because of the absence of the microscopic information of the spins in Co ions. Nonetheless, in $[\text{Ca}_2\text{CoO}_{3-\delta}]_{0.62}[\text{CoO}_2]$, it cannot be a canted-SDW as that found in $\text{Na}_{0.75}\text{CoO}_2$ ^{25,26} because the spin moments of both SDW and ferrimagnetism are along c-axis and cannot be detected in the $[\text{CoO}_2]$ planes according to $\mu^+\text{SR}$ and susceptibility experiment. Also it is very difficult to expect the $[\text{Ca}_2\text{CoO}_{3-\delta}]_{0.62}[\text{CoO}_2]$ with in-plane ferroamgnetic order and a SDW modulation perpendicular to the planes as proposed by another authors in $\text{Na}_{0.75}\text{CoO}_2$ ²⁴ because of the misfit structure between $[\text{Ca}_2\text{CoO}_{3-\delta}]$ and $[\text{CoO}_2]$ subsystems. Another possible picture is that the SDW order is ferromagnetic, while the SDW order is basically antiferromagnetic. Thus, a macroscopic magnetism should be ferrimagnetic, as actually observed below 19 K. Co-NMR and neutron-scattering experiments are desired to make out the exact magnetic structure of $[\text{Ca}_2\text{CoO}_{3-\delta}]_{0.62}[\text{CoO}_2]$.

V. CONCLUSION

To summarize, the in-plane resistivity was measured in $[\text{Ca}_2\text{CoO}_{3-\delta}]_{0.62}[\text{CoO}_2]$ single crystals in magnetic fields up to 14 T. The zero field $\rho_{ab}(T)$ exhibits a minimum and

T_{\min} increases with decreasing the oxygen content, indicative of the enhancement of SDW. The SDW strongly depends on the carrier concentration or oxygen content. Large negative MR is observed for all crystals. While a field-induced IM transition in high magnetic field were observed only in the crystal annealed in oxygen atmosphere. These results suggests there is ferromagnetic correlation in the system and the correlation is enhanced by increasing oxygen content and magnetic field. The strong effect of oxygen content on the transport and magnetotransport behavior implies that both the SDW and ferrimagnetism locate within the conducting $[\text{CoO}_2]$ sheets.

VI. ACKNOWLEDGEMENT

This work is supported by the grant from the Nature Science Foundation of China and by the Ministry of Science and Technology of China (Grant No. nkbrsf-g1999064601), the Knowledge Innovation Project of Chinese Academy of Sciences.

* Electronic address: chenxh@ustc.edu.cn

-
- ¹ A. C. Masset, C. Michel, A. Maignan, M. Hervieu, O. Toulemonde, F. Studer, B. Raveau, and J. Hejtmanek, Phys. Rev. B **62**, 166 (2000).
 - ² A. Maignan, S. Hèbert, M. Hervieu, C. Machel, D. Pelloquin and D. Khomskii, J. Phys.: Condens. Matter **15**, 2711 (2003).
 - ³ D. Pelloquin, A. Maignan, S. Hèbert, C. Martin, M. Hervieu, C. Michel, L. B. Wang and B. Raveau, Chem. Mater. **14**, 3100 (2002).
 - ⁴ T. Yamamoto, K. Uchinokura, and I. Tsukada, Phys. Rev. B **65**, 184434 (2002).
 - ⁵ T. Valla, P. D. Johnson, Z. Yusof, B. Wells, Q. Li, S. M. Loureiro, R. J. Cava, M. Mikamik, Y. Morik, M. Yoshimurak, and T. Sasakik, Nature **417**, 627 (2002).
 - ⁶ I. Tsukada, T. Yamamoto, M. Takagi, and T. Tsubone, J. Phys. Soc. Jpn. **70**, 834 (2001).
 - ⁷ S. Hèbert, S. Lambert, D. Pelloquin and A. Maignan, Phys. Rev. B **64**, 172101 (2001).
 - ⁸ K. Takada, H. Sakurai, E. Takayama-Muromachi, F. Izumi, R. A. Dilanian, and T. Sasaki, Nature **422**, 53 (2003).
 - ⁹ M. L. Foo, Y. Y. Wang, S. Watauchi, H. W. Zandbergen, T. He, R. J. Cava, and N. P. Ong, Phys. Rev. Lett. **92**, 247001 (2004).
 - ¹⁰ Y. Y. Wang, N. S. Rogado, R. J. Cava, and N. P. Ong, Nature **423**, 425 (2003).
 - ¹¹ R. Funahashi, I. Matsubara, H. Ikuta, T. Takeuchi, U. Mazutani, and S. Sodeoka, Jpn. J. Appl. Phys. Part **2** **39**, L1127 (2000).
 - ¹² J. Sugiyama, H. Itahara, T. Tani, J. H. Brewer, and E. J. Ansaldo, Phys. Rev. B **66**, 134413 (2002); J. Sugiyama, C. Xia, and T. Tani, *ibid* **67**, 104410 (2003); J. Sugiyama, J. H. Brewer, E. J. Ansaldo, H. Itahara, K. Dohmae, Y. Seno, C. Xia, and T. Tani, *ibid* **68**, 134423 (2003).
 - ¹³ M. Mikami, S. Ohtsuka, M. Yoshimura, Y. Mori, T. Sasaki, R. Funahashi, and M. Shikano, Jpn. J. Appl. Phys. **42**, 3549 (2003).
 - ¹⁴ M. Karppinen, H. Fjellag, T. Konno, Y. Morita, T. Motohashi, and H. Yamauchi, Chem. Mater. **16**, 2790 (2004).
 - ¹⁵ *Colossal Magnetoresistive Oxides*, Edited by Y. Tokura (Gordon and Breach Science Publishers, 2000), pp. 1.
 - ¹⁶ I. O. Trayanchuk, A. N. Chobot, D. D. Khalyavin, R. Szymczak, and H. Szymczak, JETP **65**, 748 (2002); M. Kopcewicz, D. D. Khalyavin, I. O. Troyanchuk, H. Szymczak, R. Szymczak, D. J. Logvinovich and E. N. Naumovich, J. Appl. Phys. **93**, 479 (2003).
 - ¹⁷ W. S. Kim, E.O. Chi, H.S. Choi, N.H. Hur, S. J. Oh, and H. C. Ri, Solid State Commun. **116**, 609 (2000).
 - ¹⁸ M. A. Senaris-Rodriguez and J. B. Goodenough, J. Solid State Chem. **118**, 323 (1995).
 - ¹⁹ N. Matsunaga, A. Briggs, A. Ishikawa, K. Nomura, T. Hanajiri, J. Yamada, S. Nakatsuji, and H. Anzai, Phys. Rev. B **62**, 8611 (2000).
 - ²⁰ K. Nomura, N. Matsunaga, A. Ishikawa, H. Kotani, K. Yamashita, T. Sasaki, T. Hanajiri, J. Yamada, S. Nakatsuji, H. Anzai, T. Nakamura, T. Takahashi, and G. Saito, Phys. Stat. sol. (b) **223**, 449 (2001).
 - ²¹ N. Biskup, S. Tomic, and D. Jerome, Phys. Rev. B **51**, 17972 (1995).
 - ²² K. Okabe, A. Miyazaki, and T. Enoki, Synth. Metals **135-136**, 693 (2003).
 - ²³ G. Gruner, Rev. Mod. Phys. **66**, 1 (1994).
 - ²⁴ A. T. Boothroyd, R. Coldea, D. A. Tennant, D. Prabhakaran, L. M. Helme, and C. D. Frost, Phys. Rev. Lett.

- 92**, 197201 (2004).
- ²⁵ J. Sugiyama, J. H. Brewer, E. J. Ansaldo, H. Itahara, T. Tani, M. Mikami, Y. Mori, T. Sasaki, S. Hébert, and A. Maignan, Phys. Rev.Lett. **92**, 017602 (2004).
- ²⁶ B. C. Sales, R. Jin, K. A. Affholter, P. Khalifah, G. M. Veith and D. Mandrus, cond-mat/0402379.
- ²⁷ T. Motohashi, R. Ueda, E. Naujalis, T. Joto, I. Terasaki, T. Atake, M. Karppinen, and H. Yamauch, Phys. Rev. B **67**, 064406 (2003).
- ²⁸ D. J. Singh, Phys. Rev. B **61**, 13397 (2000).
- ²⁹ D. J. Singh, Phys. Rev. B **68**, 020503 (2003).
- ³⁰ T. Mizokawa, L. H. Tjeng, P. G. Schultze, G. A. Sawatzky, N. B. Brooks, I. Tsukada, T. Yamamoto and K. Uchinokura, Phys. Rev. B **64**, 115104 (2001).
- ³¹ J. L. Luo, N. L. Wang, G.T. Liu, D.Wu, X. N. Jing, F. Hu, and T. Xiang, Phys. Rev. Lett. **93**, 187203 (2003).